Estimation of the minimum fluidisation velocities in well-mixed bi-disperse fluidised beds

M.A.Gilbertson

Department of Mechanical Engineering, University of Bristol, University Walk, Bristol, BS8 1TR, United Kingdom. Tel. +44 117 3315923

Abstract

A method for estimating minimum fluidisation velocities in a well-mixed, bi-disperse fluidised bed of spherical particles is described where a drag model is combined with a particle packing model. The method described does not require empirical input about a specific particle mixture, and so these minimum fluidisation velocities can be estimated over wide ranges of size and density ratios. The treatment is fully non-dimensionalised. It is shown that two minimum fluidisation velocities may be defined for a well mixed bi-disperse bed: the gas speed at which fluidisation initiates determined from considering the bed as a whole, and a higher one corresponding to the balance of forces on an individual particle. The differences between bi- and mono-disperse beds are the change in particle volume fraction owing to packing, the difference in drag around individual particles compared with the average drag, and the action of the hydrostatic pressure gradient. The latter two effects tend to increase the difference between the two limits of minimum fluidisation velocity, while packing decreases it and intensifies the dependence on mass fraction of the minimum fluidisation velocities. The influence of inertia is determined from particle properties through an Archimedes number. Though the inertial effects are not large for a wide range of particles, they can start to dominate other influences on the minimum fluidisation velocities as particle diameter increases.

Keywords: fluidisation, minimum fluidisation velocity, bi-disperse

Email address: m.gilbertson@bristol.ac.uk (M.A.Gilbertson)

1. Introduction

There is a long history of interest in the minimum fluidisation velocity, u_{mf} for when a bed consists of two well-mixed sets of particles of different densities and sizes. This has been of particular recent interest because of its relevance to biomass combustion and gasification where relatively large and light biomass particles must be well-mixed with inert material particles and the bed must be fully fluidised [1]. Classical approaches to estimating the minimum fluidisation velocity in a bi-disperse bed is summarised by [2]. One approach has been to empirically fit to experimental data, for example, Cheung *et al.*[3]. Another approach has been to calculate the minimum fluidisation velocities for bi-disperse beds in the same manner as a mono-disperse bed with particle densities and diameters averaged in some manner to reflect the bi-disperse nature of the bed. For example, Goossens *et al.*[4] calculated the overall particle density and an average particle diameter that has the equivalent total surface area per unit weight. These quantities were then used in the Wen and Yu equation [5] to calculate u_{mf} as for mono-disperse fluidised beds. Subsequent developments of this method for specific applications have tried to improve correlations through adjustments to the numerical coefficients in the equation e.g. [6–8].

It became apparent that the estimation of the point of minimum fluidisation in bi-disperse beds is more complex than for mono-disperse beds beyond accounting for changes to the overall bed parameters. The estimated values of u_{mf} for a bi-disperse bed could vary from experimental measurements by as much as $\pm 40\%$ [6, 7]. There are a number of issues that might account for this.

First, from measurements of pressure drop against velocity, it is apparent that in a bi-disperse bed fluidisation is not a single event that is the crossing of a threshold, but is a process that continues over a range of gas velocities [7, 9–11]. This results in the definition of two minimum fluidisation velocities, one at which fluidisation initiates and a higher one that corresponds to the gas speed at which the pressure drop over a bed reaches a maximum. This has been accounted for as a result of the segregation of particles above the initial minimum fluidisation velocity up to a gas speed above which the pattern of segregation becomes independent of gas speed.

The second issue that gives rise to uncertainty in estimating minimum flu-

idisation velocities is that when a bed consists of particles of different sizes, it is possible for the smaller particles to pack the interstices between the large ones [12, 13]. Drag is strongly dependent on particle volume fraction, ϕ, which can vary markedly with the degree of packing that the particle geometry allows and the proportion of each of the bed components [9, 13]. There has been success at estimating the initial minimum fluidisation velocity for bi-disperse beds by measuring ϕ directly and then calculating u_{mf} using the viscous term of the Ergun equation with mixture particle density and diameter [9, 14]. An alternative approach has been to use curve fitting for empirical measurements of minimum fluidisation velocity to account for the effect of packing [3, 13]. As well as ϕ, the packing of small particles between the large ones will affect the nature of the channels through which the fluidising gas passes through a bi-disperse bed and hence the drag exerted on the particles [15].

A third issue is the exertion of hydrostatic forces as well as drag on particles in a fluidised bed. This is straightforward to allow for in a mono-disperse bed, but in a bi-disperse bed for which the densities of the two components are different, the hydrostatic force on a particular particle depends on the proportion of each component, and this can be difficult to account for [16].

In this paper, a method is presented for estimating minimum fluidisation velocities in well-mixed bi-disperse fluidised beds of spherical particles that explicitly includes all their physical features without requiring empirical measurements of a particular bed. A drag model [15, 17] is combined with the estimation of ϕ through the use of a packing model [18], and the effects of the hydrostatic pressure gradient and inertia are included. The resulting equations are fully non-dimensionalised,so the results are generally applicable. The model is applied at two scales: that of the overall bed, and that of the individual particle. Several drag models are available, but that of Hoef *et al.* [15, 17] is used as it allows the identification of specific physical mechanisms for the generation of drag, and for drag to be calculated at both scales. This drag model has been used successfully elsewhere to model fluidised beds e.g. [19–21]. The results from this paper show the degree of complexity introduced into the process of fluidisation by a second particle component.

2. Minimum fluidisation velocities in mono-sized fluidised beds

The minimum fluidisation velocity for a mono-sized bed of particles, u_{mf_0}, is the speed of a fluid flow though it, u_g, at which the particles' weight is matched by the fluid forces acting upon them: drag and hydrostatic pressure. The drag force can be written down as the Stokes drag on an isolated particle multiplied by the factor F that accounts for the effect of surrounding particles and inertia on the drag on a particle in a bed [17]. F is a function of ϕ_0, the particle volume fraction for a mono-disperse bed, and Re, the particle Reynolds number. It can be shown that the net force generated on a particle of diameter d_0 when the hydrostatic pressure gradient is taken into account is the drag force divided by $1-\phi_0$ [15]. When the bed is fully fluidised and the gas density is much less that that of the particles, $\rho_g \ll \rho_0$, the force balance on a representative particle is

$$3\pi\mu d_0 u_g F + \phi_0 \rho_0 \frac{\pi}{6} d^3 g = \rho_0 \frac{\pi}{6} d_0^3 g, \tag{1}$$

where the first term is fluid drag and the third term is the weight of the particle. The second term is the hydrostatic force exerted on the particles owing to the supspension of the bed. [15].

In non-dimensional form [15]

$$\frac{F}{1-\phi_0} u^*_{mf} = 1, \tag{2}$$

where

$$u^*_{mf} = u_{mf}/u_{t0}, \tag{3}$$

a type of Stokes number, and

$$u_{t0} = \frac{\rho_0 d_0^2 g}{18\mu} \tag{4}$$

is the terminal velocity of an isolated particle experiencing Stokes drag.

The correction F to the fluid drag can be divided into two parts, one viscous and one inertial [17], so that

$$F = F_v(\phi) + F_{Re}(\phi, Re). \tag{5}$$

From the results of lattice Boltzmann simulations of flows through arrays of particles, an expression for the low-Reynolds number correction F_v has been

proposed [15] and, for higher Reynolds numbers another for F_{Re} that has an accuracy of 10% when $Re = 1000$ [17].

When a bed is viscously dominated, then u^*_{mf} is equal to a constant that is a function of ϕ and information about a specific bed is introduced when scaling is removed. When inertia is significant then F is a function of Re as well as ϕ. Re may be expressed as $Re = Ar\, u^*_{mf}$ where

$$Ar_0 = \frac{\rho_g \rho_0 d_0^3 g}{18\mu^2}, \tag{6}$$

is a Archimedes number describing the ratio between the weight of a particle and the viscous drag acting on it in a monodisperse bed when $\rho_g \ll \rho_0$. Eqn (2) can then be solved for u^*_{mf}. When viscous forces dominate then u^*_{mf} is a constant; when inertial forces are significant, then u^*_{mf} has to be found from the implicit solution of Eqn (2).

3. Minimum fluidisation velocities in well-mixed bi-disperse beds

For a bi-disperse mixture of particles, s will denote the 'small' diameter particles, l the 'large' diameter particles, and i denotes either component. The amount of small particles is denoted by the mass fraction x.

The average density for the bed is

$$\frac{1}{\rho_{av}} = \frac{x}{\rho_s} + \frac{1-x}{\rho_l}. \tag{7}$$

Two density ratios may be defined:

$$w = \frac{\rho_s}{\rho_l}; \quad z_i = \frac{\rho_i}{\rho_{av}}. \tag{8}$$

The Sauter diameter is a suitable average diameter [15],

$$\frac{1}{d_{av}} = \frac{x/z_s}{d_s} + \frac{(1-x)/z_l}{d_l}. \tag{9}$$

Two size ratios are defined as

$$r = \frac{d_s}{d_l}; \quad y_i = \frac{d_i}{d_{av}}. \tag{10}$$

All the particles in this article are assumed to have Geldart group-B behaviour i.e. ϕ_0 is independent of u_g.

3.1. Forces on a bed as a whole

For the whole bed, the minimum velocity at which fluidisation initiates may be defined as that at which it ceases to act as a static bed, u_{mf_1}. This will be when the weight of the entire fixed bed of particles is just matched by the fluid forces upon it [9, 12]. In a fixed bed, forces are transmitted directly from one particle to another, and so the bed may be considered in bulk. The same framework for expressing drag as for a mono-disperse bed of particles may be employed with Re based on an average, representative particle so that in dimensionless terms, when the weight of the bed in bulk is fully supported by the gas flow,

$$\left[F_v(\phi) + F_{Re}(\phi,\, Ar_{av}\, u^*_{mf_1})\right] \frac{u^*_{mf_1}}{1-\phi} = 1. \tag{11}$$

where $u^*_{mf_1} = u_{mf_1}/u_{t_{av}}$ is the dimensionless minimum fluidisation velocity for the whole bed. $u_{t_{av}}$ and Ar_{av} are based on d_{av} and ρ_{av}. This is the equivalent of the expression for the initial minimum fluidisation velocity in [9], though there the drag is based on the Carmen-Kozeny equation. As for Eqn (2), the ϕ in the denominator arises because of the hydrostatic force generated by the suspension of all the particles.

3.2. Fluidisation based on forces on individual particles

In a well-mixed, bi-disperse bed not all of the particles will be fully fluidised when $u^*_{mf_1}$ is exceeded. On one of the components the force exerted on a particle will be more than that necessary to fluidise it, but on the other component it will be less. When the particles are in contact, the excess force from the former component can be transmitted to the latter; however, if a well-mixed bed is to be fully fluidised, the particles should not be in sustained contact with each other and each particle must be supported individually by the gas flow [22]. To determine the gas velocity at which this takes place, the forces exerted by the gas flow on an individual particle must be considered. This will define an upper fluidisation velocity, u_{mf_2}, expressing the minimum gas velocity for the weight of the particle to be supported in a fully-fluidised, well-mixed bed.

The gas velocity at which an individual particle's weight is supported will depend on its characteristics, not the average ones for the bed. There are

also two important differences between the forces on individual particles in bi-disperse beds and the force on an average particle.

First, when a bi-disperse system is considered at the bed-scale, the average non-dimensional drag on a particle is equivalent to the non-dimensional drag on a particle in a mono-disperse bed with the same ϕ; however, when an individual particle is considered, this is not true [15]. Through lattice-Boltzmann simulations, it has been shown that for bi-disperse beds of spherical particles, this may be expressed by multiplying F by a factor [15]

$$F_{p_i} = \left((1-\phi)\, y_i + \phi y_i^2 \right). \tag{12}$$

A better fit with simulation results can be found with the addition to Eqn (12) of $0.064\,(1-\phi)\,y_i^3$ [15]; however, this was at the expense of drag no longer taking on the values for mono-disperse beds when $x = 0$ or $x = 1$ [15] and the benefit is only significant for values of ϕ much smaller than those found in dense fluidised beds [15].

The second difference is the action of the pressure gradient. In a bi-disperse bed, when individual particles are considered there is cross-coupling in the momentum balance for a particle as the total force acting on a particle of one-component will depend on the force exerted by the fluid on the particles of the other component. For a general description of bi-disperse particle systems, this is a difficult problem [16]; however, for a fully-fluidised bed, it can be overcome as the pressure gradient can be equated to the weight of particles in the whole bed so that it has the value $-\phi\rho_{av}g$. For particles of different sizes but equal densities in a fully-fluidised bed, the total force on a particle will be the drag force divided by $(1-\phi)$, in a similar manner to mono-sized particles.

For a particle of component i, the velocity at which fluid forces equals the weight of an individual representative particle of component i, $u_{mf\,2i}$ in a bi-disperse bed is given by the force balance per unit weight for the particle,

$$F_{p_i}\,(F_v + F_{Re})\,\frac{u_{mf\,2i}}{u_{ti}} + \phi\frac{\rho_{av}}{\rho_i} = 1. \tag{13}$$

The first term on the left-hand side expresses drag, the second term is buoyancy, and the right-hand side is particle weight. Converting to non-dimensional variables and using Eqn (12),

$$u^*_{mf\,2i} = \frac{1}{F_v + F_{Re}}\,(z_i - \phi)\left(\frac{y_i}{(1-\phi) + \phi y_i}\right) \tag{14}$$

or when viscous forces dominate, from Eqn (11)

$$u^*_{mf_{2i}} = u^*_{mf_1} \left(\frac{z_i - \phi}{1 - \phi} \right) \left(\frac{y_i}{(1-\phi) + \phi y_i} \right). \tag{15}$$

The first term in brackets corresponds to the effect of buoyancy and the second term the effects of the difference between the diameter of the particle being considered and d_{av}.

Characterising a bi-disperse fluidised bed with $u_{mf_{2i}}$

$u^*_{mf_{2i}}$ can be defined for a particle from either component of a bi-disperse mixed bed. Only will it have physical meaning when the entire bed is fully fluidised, otherwise the buoyancy term in Eqn (13) is incorrect; therefore, for a particular value of x, the larger value of $u^*_{mf_{2i}}$ characterises the minimum velocity at which a mixed fluidised bed is fully fluidised (denoted as $u^*_{mf_2}$); the value for the other component does not have physical meaning.

Which component defines $u^*_{mf_{2i}}$ depends on r and w, with the density ratio having the greater influence. When the larger component is also the denser ($w < 1$), $u^*_{mf_2} = u^*_{mf_{2l}}$ always. When the small particles are the denser ($w > 1$) then for any r there will be a limiting value of w below which the larger, less-dense particles may define $u^*_{mf_2}$ rather than the smaller, denser ones. The ranges over which this are true for when inertial effects are negligible is shown in Fig. 1. Even for very large differences in the diameters of the two components, the larger, less-dense particles define $u^*_{mf_2}$ only when x is small or when w is not much more than 1.

4. Scaled results

For bi-disperse fluidised beds, two minimum fluidisation velocities may be found: $u^*_{mf_1}$ for when fluidisation initiates, and $u^*_{mf_2}$ for when a well-mixed, bi-disperse bed can be completely fluidised. Particle shape is not investigated here, so in a bi-disperse bed the particles may differ in size and density. The simplest case that can be used to examine the effects of these properties is when r is large so that ϕ is not a function of x and a bi-disperse bed acts in a similar way to a mono-disperse bed. When the difference in size of particles is sufficiently large for $\phi = f(x)$, then the behaviour of the bed with respect

to the minimum fluidisation velocities changes. A further complication will be the effect of inertial forces when they are large enough to be significant. Each of these cases will be examined in turn and, through the use of scaled parameters, for bi-disperse fluidised beds in general. There will then be an example showing how the scaled parameters relate to unscaled velocities and how the other factors described here affect minimum fluidisation velocity when compared with the primary scaling found in mono-disperse fluidised beds.

4.1. Minimum fluidisation velocities in beds where ϕ is fixed and viscous drag dominates

For particles of a similar shape, when $r > 0.741$ the mixture of two bed components has the same particle volume fraction mixed as when they are unmixed, $\phi = \phi_0$ [23]. The minimum fluidisation velocities for these conditions are shown in Fig. 2. Taken as a whole, such a bed is analogous to a mono-disperse bed of particles with average properties so that when viscous forces dominate, $u^*_{mf_1}$ has a fixed value given by Eqn (2), which has a value of 0.0106 when $\phi = 0.60$. $u^*_{mf_2}$ increases with x owing to the effect of the hydrostatic pressure gradient. $r = 1$ corresponds to the special case when bed components have the same size, but different densities. When $w > 1$ (i.e. the smaller particles are also the denser), a similar result to that shown in Fig. 2 is obtained except that the line describing $u^*_{mf_2}$ is reversed.

4.2. The effect of particle packing

When $r < 0.741$, small, spherical particles can pack the interstices between the large particles in a bi-disperse bed and $\phi = \phi(x)$ and can be significantly larger than ϕ_0 [23]. This can greatly affect the values of the scaled minimum fluidisation velocities.

Packing behaviour in bi-disperse beds can be estimated without the use of empirical measurements of specific mixtures of particles through the use of a packing model. The linear-mixture model [18] combines a linear model [24] for when $r < 0.154$, the point at which small spherical particles can move through the interstices of large ones without disturbing them, with a mixture model [25] for when $0.154 < r < 0.741$. The mixture model is appropriate when the values of ϕ_0 for each component are equal, but if the particles for each component have

different shapes then a fully linear model must be used instead [18]. This model has been experimentally validated [18, 23, 25].

Mixture particle volume fractions depend on the partial volume fraction of the small particles X where

$$X = \frac{x}{x + w(1-x)}. \tag{16}$$

For a binary mixture of spherical particles when $\phi_{0_s} = \phi_{0_l} = \phi_0$, when $r \geq 0.741$, then $\phi = \phi_0$. When $0.154 \leq r < 0.741$, then the particle volume fraction is determined by mixing and [24]

$$1/\phi = 1/\phi_0 + (1-X)X\left(\beta + \gamma\left(1-2X\right)\right) \tag{17}$$

where

$$\beta = 10.288 \times 10^{-1.4566\phi_0}\left(-1.002 + 0.1126r + 5.8455r^2 - 7.9488r^3 + 3.1222r^4\right) \tag{18}$$

$$\gamma = \left(-1.3092 + 15.039\phi_0 - 37.453\phi_0^2 + 40.869\phi_0^3 - 17.11\phi_0^4\right) \left(-1.0029 + 0.3589r + 10.970r^2 - 22.197r^3 + 12.434r^4\right). \tag{19}$$

When $r < 0.154$ then the particle volume fraction is dominated by unmixing. An overall particle volume fraction can be calculated [26] for both components and the lower value is taken to represent the mixture where

$$\phi_0/\phi_l = (1-X) + (1-f(r))X; \tag{20}$$

$$\phi_0/\phi_s = X + (1-(1-\phi_0)g(r))(1-X), \tag{21}$$

where the interaction coefficients are given by

$$f(r) = (1-r)^{3.3} + 2.8r(1-r)^{2.7} \tag{22}$$

$$g(r) = (1-r)^{2.0} + 0.4r(1-r)^{3.7}. \tag{23}$$

The inset for Fig. 3a shows the computed increase in ϕ for the values of r examined.

(24)

(25)

The effect of the packing of small particles between the large ones is shown in Fig. 3a where $w = 1$ i.e. the bed is a mixture of particles of two different sizes, but the same density. There are two main effects of r on the values of the two minimum fluidisation velocities. First, $u^*_{mf_1} \neq u^*_{mf_2}$ and the difference between the two scaled minimum fluidisation velocities increases with x, driven by the difference between d_l and d_{av}. The second effect is that the shape of the scaled minimum fluidisation curves is substantially changed by the increase in the value of ϕ when $r < 0.741$ and decreases. $u^*_{mf_1}$ is no longer a constant, but has a minimum whose value and the corresponding value of x decrease as r is reduced. When r is small, the effects of packing are dominant so that the dependence on x of $u^*_{mf_2}$ is changed from a consistent rise to being pulled down close to the line for $u^*_{mf_1}$.

Fig. 3b shows the fluidisation curves when $w = 0.5$ i.e. the larger particles are also denser. The strong divergence between $u^*_{mf_1}$ and $u^*_{mf_2}$ with increasing x caused by the hydrostatic gradient (as seen in Fig. 2) is superimposed on the shape of the curves generated by packing shown in Fig. 3a.

Fig. 3c shows the fluidisation curves when the smaller particles are more dense than the larger ones ($w > 1$). The dependence of hydrostatic pressure on x is simply reversed; however, the effects of packing are not, which results in very different dependencies of the scaled minimum fluidisation velocities on x. When $w > 1$, it is possible for $u^*_{mf_2}$ to be defined by the less-dense component, but particle packing restricts this effect as shown in Fig. 1.

In Fig. 3a the value of $u^*_{mf_2}$ does not converge on the value of $u^*_{mf_s}$ when $x = 1$. This is because $u^*_{mf_2} = u^*_{mf_{2l}}$ so that the limiting case as $x \to 1$ is of a single large particle in a bed of small particles. From Eqn (15), the fluid force required to suspend a large particle will exceed that for the small particles and so $u^*_{mf_2} > u^*_{mf_s} = u^*_{mf_1}(x = 1)$. The same is true for Fig. 3b; however, for Fig. 3c, $u^*_{mf_2} = u^*_{mf_{2s}}$, and so when $x = 0$, $u^*_{mf_2} > u^*_{mf_l} = u^*_{mf_1}(x = 0)$.

4.3. The effect of inertial forces

Inertia has the effect of increasing the scaled drag experienced by particles and reducing the scaled minimum fluidisation velocities. When the bed is considered as a whole and $u^*_{mf_1}$ is calculated, the same framework as for a monodisperse bed may be employed with the effect of inertia characterised by the

Archimedes number Ar_{av} (defined by Eqn (6)) based on the average particle density and diameter. Its influence on $u^*_{mf_1}$ for a bi-disperse mixture where $\phi = \phi_0$ is shown in Fig. 4. The value of $u^*_{mf_1}$ begins to significantly deviate from the value for when inertia is negligible when Ar_{av} has a value of a few hundred. For an idea of a physical meaning of the value of the Archimedes number, $Ar = 500$ for glass particles ($\rho_p = 2500\,\mathrm{kg/m^3}$) fluidised by air when $d_p = 445\,\mu\mathrm{m}$.

Ar_{av} is based on the average particle diameter quantities and so for most cases diminishes as x becomes larger. This means that even in beds where the larger component is large and heavy, inertial forces may not be significant over large ranges of x when w is small. The dependency of Ar_{av} on d_{av} means that it is no longer possible to plot a completely general variation of the minimum fluidisation velocities with x. Fig. 5 shows the variation of the minimum fluidisation velocities with x for several values of r for a value of Ar_s selected so that inertia is always important, even at high x. Comparison with Fig. 3c shows that the effect of inertial forces is to increase drag, particularly at low x and to reduce the effects of packing on the minimum fluidisation velocities.

5. Unscaled results

It has been shown above that in bi-disperse fluidised beds, it is possible for r and w to cause significant variation from the values of the scaled minimum fluidisation velocity that would be expected from considering equivalent single-component fluidised beds. However, the dominant scaling in fluidised beds is between the weight and the fluid forces acting upon a particle, and in a bi-disperse bed this is expressed by $u_g/u_{t_{av}}$. Figure 6 compares the scaled and unscaled minimum fluidisation velocities for the particles whose properties are summarised in Tab. 1. The principle scaling in a fluidised bed between weight and drag is evident. When a bi-disperse fluidised bed behaves as a single-component fluidised bed, then from Eqns (2) and (4), the minimum fluidisation velocity is inversely proportional to $\rho_{av} d^2_{av}$, which gives rise to an exponential decrease in minimum fluidisation velocities with x. When r is small, then increased packing very much intensifies the variation with x. The result is a very steep drop in minimum fluidisation velocities with x and which then have nearly

constant values over large ranges of the higher values of x.

6. Discussion and conclusion

The method for estimating minimum fluidisation velocities in well-mixed, bi-disperse fluidised beds of spherical particles described here does not require any empirical measurements for a particular bed. The equations are also non-dimensionalised and so are applicable to any bed for which the constituent models may be applied.

There are two scales that may be considered for a fluidised bed: the overall bed scale and that of individual particles. In a mono-sized bed these two scales can be reconciled in that it is the point of minimum fluidisation is considered to be the point at which the forces on all of the individual particles balance and this is manifest at the bed-scale by the pressure drop over the bed reaching a maximum with respect to gas speed. For the whole-bed scale, the minimum fluidisation velocity u_{mf_1} is the initial minimum fluidisation velocity that has been defined previously e.g. [3, 10, 27]. The results for u_{mf_1} compare well with classical predictions of the minimum fluidisation velocity for large r when there is no packing of the small particles between the large ones, as shown in figure 7a. When r is small, Figs 7b and 7c, the packing of the particles has a significant effect on the expected values of u_{mf_1}, resulting in significant deviations. The correlation of Noda *et al.* [6] was developed specifically for beds with a small value of r, but does not appear to offer great advantages over the simpler correlations. The packing model can be adapted to allow for more than two components and also differently shaped particles [18], but the degree of the challenge of this is shown by the predictions of a correlation that was developed specifically for beds containing biomass particles, which are also likely to be segregating strongly [8]. Though it was able to estimate the minimum fluidisation velocities for the specific situation that it was developed for, it deviates a great deal from other drag-model based predictions not specifically prepared for biomass systems.

In a well-mixed bi-disperse bed, the bed-scale minimum fluidisation velocity does not correspond to the gas speed at which the forces an individual particle balance because it is determined by the balance of forces on the particle, includ-

ing buoyancy, which is determined by the density ratio, and a factor accounting for the difference between drag on an individual particles and the average drag, determined by the size ratio. This gives rise to a higher fluidisation velocity, u_{mf_2}. This is different from the final minimum fluidisation velocity defined previously e.g. [3, 10, 27], which describes the higher gas velocity that would enable segregation to fully take place and the bed to become steady state: u_{mf_2} applies to a well-mixed bed and so is not associated with segregation nor with the bed being in a transient state. This is likely to be particularly important in applications for which x is large, such as biomass combustion and gasification where a bed may appear to fluidised as a whole, but individual particles may not be.

The point at which the weight of all the particles in most practical bi-disperse beds is supported is difficult to predict because of the propensity for many beds to segregate. Many forms of segregation have been observed, and bi-disperse beds can segregate into regions containing different proportions of the two bed components e.g. [28]. The propensity of fluidised beds to segregate readily is explained by the fact that even in well-mixed beds, there is a region between u_{mf_1} and u_{mf_2} where the bed is no longer static as a whole, but the different magnitudes of the forces acting on particles in each component can cause segregation [20, 22]. The overall segregation pattern will depend on the balance between mixing and segregation processes within a specific bed [29]. Furthermore, segregation takes place on a different scales, and small scale regions of different composition to their surroundings may form [30, 31]. When r is small, the minimum fluidisation velocities change sharply with x and so as segregation takes place, the gas velocity necessary to fluidise a region can markedly change. The minimum fluidisation velocity measured for a particular bed taken as a whole will then often be difficult to predict as its structure would be the result of the interaction of several processes that depend on local conditions. Segregation makes experimental validation of u_{mf_2} difficult to do for most particle mixtures, and may account for the large errors previously encountered when expressions for u_{mf} are compared with experimental data. However, the criteria described here for predicting minimum fluidisation velocities can be applied to any region within a segregated bed that is uniformly well mixed, and they

may be used to predict their formation and the development of segregation in different mixtures of particles.

The influence of inertia on the minimum fluidisation velocities can be characterised by Ar_{av}. This has an advantage over using Re in that it requires only the particles' properties for its calculation. Inertia becomes significant when Ar_{av} has a value of a few hundred, which means that for many practical beds the effects of inertia are not large; however, when they do become significant, they increase rapidly with increasing diameter.

Acknowledgements

This work was undertaken during a University Research Fellowship awarded by the Institute of Advanced Study at the University of Bristol. This research did not receive any specific grant from funding agencies in the public, commercial, or not-for-profit sectors.

Nomenclature

Roman letters

Ar Archimedes number defined by Eqn (6) [-]

d Particle diameter [m]

F Correction for drag for the presence of other particles [-]

F_v Viscous correction for drag for the presence of other particles [-]

F_{Re} Inertial correction for drag for the presence of other particles [-]

F_p Correction to drag to take into account hydraulic radius for flow around a particular particle [-]

r Ratio of diameters of small to large particles [-]

Re Particle Reynolds number [-]

u_g Superficial gas velocity [m/s]

u_{mf_1} Initial minimum fluidisation gas velocity [m/s]

u_{mf_2} Complete minimum fluidisation gas velocity [m/s]

$u^*_{mf_1}$ Non-dimensional initial minimum fluidisation gas velocity [-]

$u^*_{mf_1}$ Non-dimensional complete minimum fluidisation gas velocity [-]

u_t Terminal speed for an isolated particle [m/s]

w Ratio of density of small to large particles [-]

x Mass fraction of small particles [-]

X Partial volume fraction of small particles [-]

y Ratio of diameter of one component to the average particle diameter [-]

z Ratio of density of one component to the average particle density [-]

Greek letters

μ Fluid viscosity [kg/m s]

ρ Density [kg/m^3]

ϕ Particle volume fraction

Subscripts

0 Value for particles in a mono-sized bed

av Average particle

g Gas

i Either component of the mixture

l Large particles

s Small particles

References

[1] H. Cui, J. R. Grace, Fluidization of biomass particles: A review of experimental multiphase flow aspects, Chemical Engineering Science 62 (2007) 45–55.

[2] S. Wu, J. Baeyens, Segregation by size difference in gas fluidized beds, Powder Technology 98 (1998) 139–150.

[3] L. Cheung, A. Nienow, P. Rowe, Minimum fluidisation velocity of a binary mixture of different sized particles, Chemical Engineering Science 29 (1974) 1301–1303. doi:10.1016/0009-2509(74)80137-5.

[4] W. Goossens, G. Dumont, G. Spaepen, Fluidization of binary mixtures in the laminar flow region, Chemical Engineering Progress Symposium Series 676 (1971) 38–43.

[5] Y. Wen, Y. Yu, Mechanics of fluidisation, Chemical Engineering Progress Symposium Series 62 (1966) 100–111.

[6] K. Noda, S. Uchida, T. Makino, H. Kamo, Minimum fluidization velocity of binary mixture of particles with large size ratio, Powder Technology 46 (1986) 149–154. doi:10.1016/0032-5910(86)80021-3.

[7] T. J. P. Oliveira, C. R. Cardoso, C. H. Ataíde, Bubbling fluidization of biomass and sand binary mixtures: Minimum fluidization velocity and particle segregation, Chemical Engineering and Processing: Process Intensification 72 (2013) 113–121.

[8] B. Paudel, Z.-G. Feng, Prediction of minimum fluidization velocity for binary mixtures of biomass and inert particles, Powder Technology 237 (2013) 134–140.

[9] B. Formisani, Packing and fluidization properties of binary mixtures of spherical particles, Powder Technology 66 (1991) 259–264.

[10] A. Marzocchella, P. Salatino, V. Di Pastena, L. Lirer, Transient fluidization and segregation of binary mixtures of particles, AIChE Journal 46 (2000) 2175–2182.

[11] B. Formisani, R. Girimonte, Experimental analysis of the fluidization process of binary mixtures of solids, KONA 21 (2003) 66–75.

[12] S. Chiba, A. Nienow, T. Chiba, H. Kobayashi, Fluidised binary mixtures in which the denser component may be flotsam, Powder Technology 26 (1980) 1–10.

[13] P. Rowe, A. Nienow, Minimum fluidisation velocity of multi-component particle mixtures, Chemical Engineering Science 30 (1975) 1365–1369.

[14] B. Formisani, R. Girimonte, T. Longo, The fluidization process of binary mixtures of solids: Development of the approach based on the fluidization velocity interval, Powder Technology 185 (2008) 97–108.

[15] M. A. van der Hoef, R. Beetstra, J. A. M. Kuipers, Lattice-Boltzmann simulations of low-Reynolds-number flow past mono- and bidisperse arrays of spheres: results for the permeability and drag force, Journal of Fluid Mechanics 528 (2005) 233–254.

[16] R. Beetstra, M. A. van der Hoef, J. A. M. Kuipers, Drag force of intermediate Reynolds number flow past mono- and bidisperse arrays of spheres–erratum, AIChE Journal 53 (2007) 3020–3020.

[17] R. Beetstra, M. A. van der Hoef, J. A. M. Kuipers, Drag force of intermediate Reynolds number flow past mono- and bidisperse arrays of spheres, AIChE Journal 53 (2007) 489–501.

[18] A. B. Yu, R. P. Zou, Prediction of the Porosity of Particle Mixtures, KONA Powder and Particle Journal 16 (1998) 68–81.

[19] R. Beetstra, M. A. van der Hoef, J. A. M. Kuipers, Numerical study of segregation using a new drag force correlation for polydisperse systems derived from lattice-Boltzmann simulations, Chemical Engineering Science 62 (2007) 246–255.

[20] F. P. Di Maio, A. Di Renzo, V. Vivacqua, Extension and validation of the particle segregation model for bubbling gas-fluidized beds of binary mixtures, Chemical Engineering Science 97 (2013) 139–151.

[21] C. M. Boyce, A. Ozel, N. P. Rice, G. J. Rubinstein, D. J. Holland, S. Sundaresan, Effective Particle Diameters for Simulating Fluidization of Non-spherical Particles: CFD-DEM Models vs. MRI Measurements, AIChE Journal 63 (2017) 2555–2568.

[22] F. P. Di Maio, A. Di Renzo, V. Vivacqua, A particle segregation model for gas-fluidization of binary mixtures, Powder Technology 226 (2012) 180–188.

[23] A. B. Yu, N. Standish, An analytical—parametric theory of the random packing of particles, Powder Technology 55 (1988) 171–186.

[24] R. P. Zou, A. B. Yu, Evaluation of the packing characteristics of mono-sized non-spherical particles, Powder Technology 88 (1996) 71–79.

[25] A. B. Yu, N. Standish, Estimation of the porosity of particle mixtures by a linear-mixture packing model, Industrial & Engineering Chemistry Research 30 (1991) 1372–1385.

[26] A. B. Yu, R. P. Zou, N. Standish, Modifying the Linear Packing Model for Predicting the Porosity of Nonspherical Particle Mixtures, Industrial & Engineering Chemistry Research 35 (1996) 3730–3741. doi:10.1021/ie950616a.

[27] B. Formisani, G. Cristofaro, R. Girimonte, A fundamental approach to the phenomenology of fluidization of size segregating binary mixtures of solids, Chemical Engineering Science 56 (2001) 109–119. doi:10.1016/S0009-2509(00)00426-7.

[28] G. G. Joseph, J. Leboreiro, C. M. Hrenya, A. R. Stevens, Experimental segregation profiles in bubbling gas-fluidized beds, AIChE Journal 53 (2007) 2804–2813. doi:10.1002/aic.11282.

[29] L. Gibilaro, P. Rowe, A model for a segregating gas fluidised bed, Chemical Engineering Science 29 (1974) 1403–1412.

[30] M. A. Gilbertson, I. Eames, Segregation Patterns in Gas-Fluidized Systems, Journal of Fluid Mechanics 433 (2001) 347–356. doi:null.

[31] A. Nermoen, C. Raufaste, S. D. deVilliers, E. Jettestuen, P. Meakin, D. K. Dysthe, Morphological transitions in partially gas-

fluidized granular mixtures, Physical Review E 81 (2010) 061305. doi:10.1103/PhysRevE.81.061305.

Figure captions

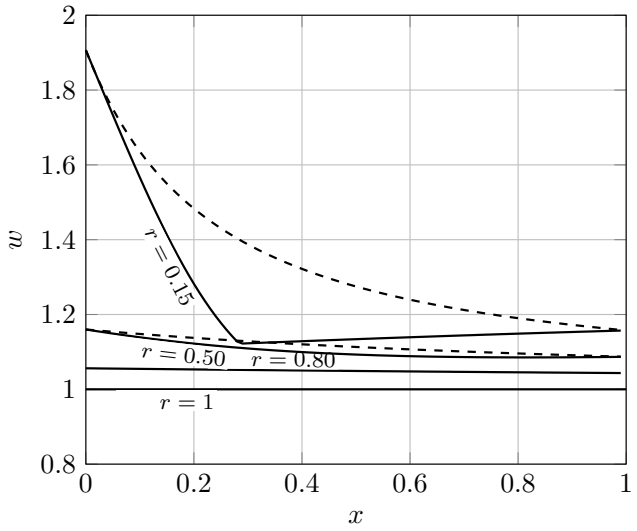

Figure 1: Figure showing the conditions when the force balance on a representative particle for the less-dense component defines u_{mf_2} for a bi-disperse bed. This only happens when $w > 1$, but also has a value that lies below the appropriate solid line in the figure. The solid lines take into account packing and the dashed lines represent the curves for fixed $\phi = \phi_0 = 0.60$, where this is different.

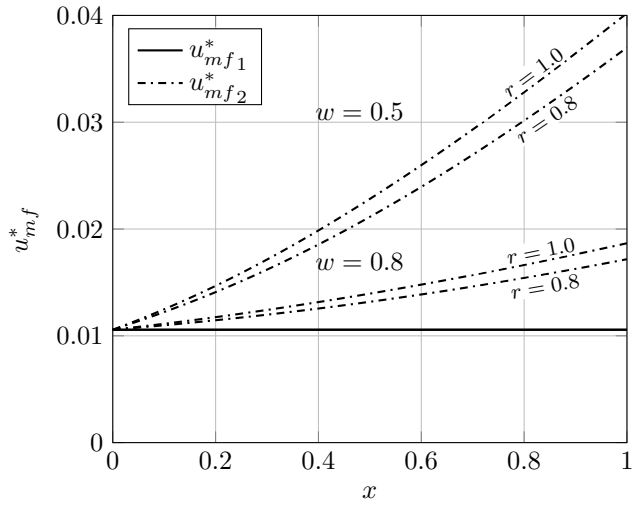

Figure 2: Minimum fluidisation velocities for bi-disperse mixtures for which $r > 0.74$ and $\phi = \phi_0$, and viscous drag dominates. For the case shown $w < 1$ and $\phi = \phi_0 = 0.60$.

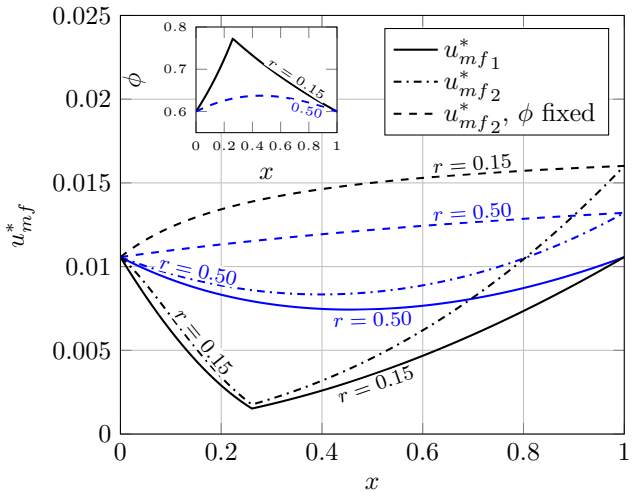

(a) $w = 1$ i.e. both components have the same density. The inset shows the computed variation in ϕ with x.

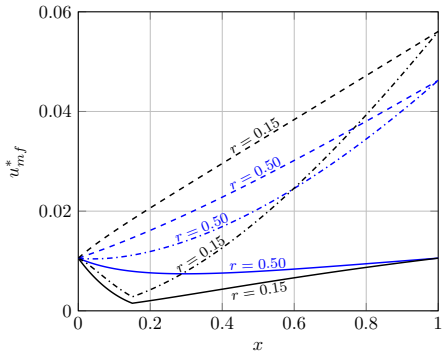

(b) $w = 0.5$ i.e. the larger particles are also denser.

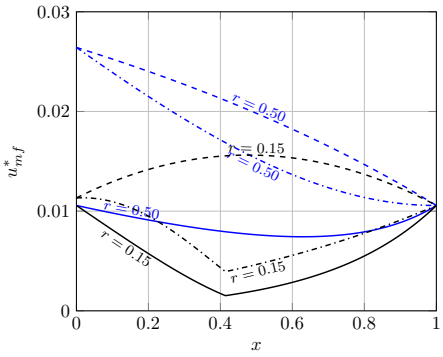

(c) $w = 2$. i.e. the smaller particles are also the denser

Figure 3: The effects of particle packing on the scaled minimum fluidisation velocities. $\phi = \phi(x)$. In all cases inertial effects are negligible and neglected.

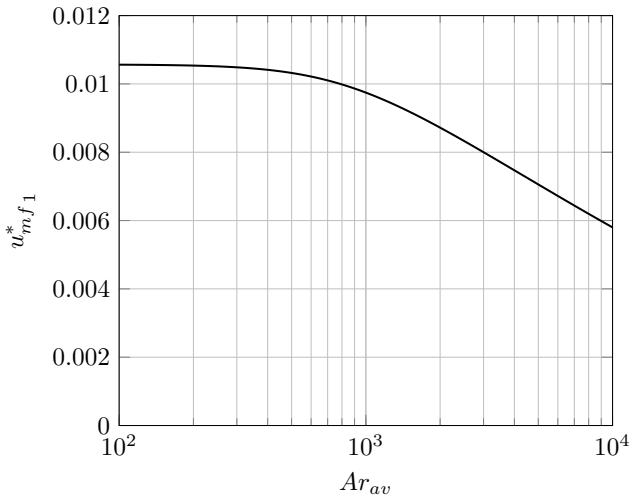

Figure 4: The effect of inertia, characterised with the Archimedes number Ar, on the scaled minimum fluidisation velocity for the whole bed, $u^*_{mf_1}$. $r > 0.74$ so $\phi = \phi_0$. $Ar_{av} = 100$ corresponds to $Re_{u_{mf_1}} = 1.1$; $Ar_{av} = 10\,000$ corresponds to $Re_{u_{mf_1}} = 58$. $\phi_0 = 0.60$.

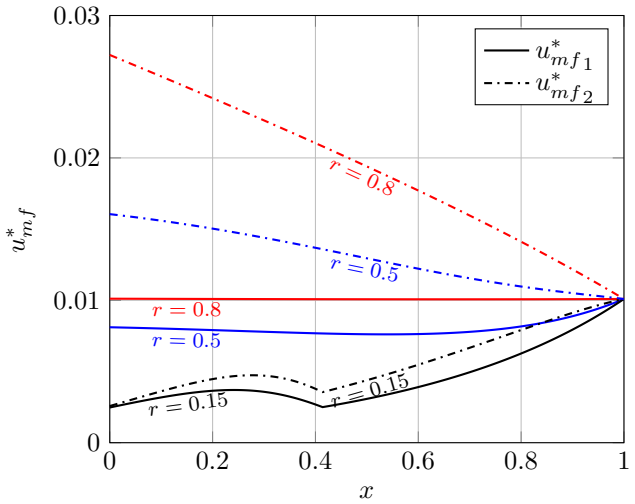

Figure 5: The effect of inertia on scaled minimum fluidisation velocities. For the smaller particles, $Ar_s = 707$, which means that inertial effects are important for all x. $w = 2$.

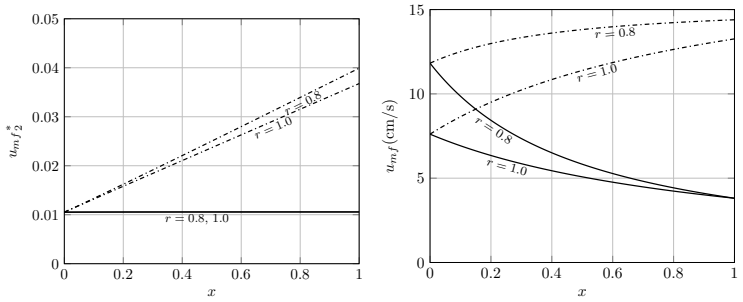

(a) (b)

$\rho_s = 1250\,\mathrm{kg/m^3}$, $w = 0.5$, $r = 0.8$ and $r = 1.0$.

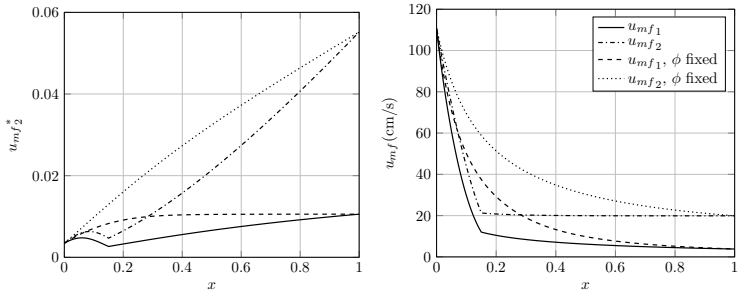

(c) (d)

$\rho_s = 1250\,\mathrm{kg/m^3}$, $w = 0.5$, and $r = 0.15$.

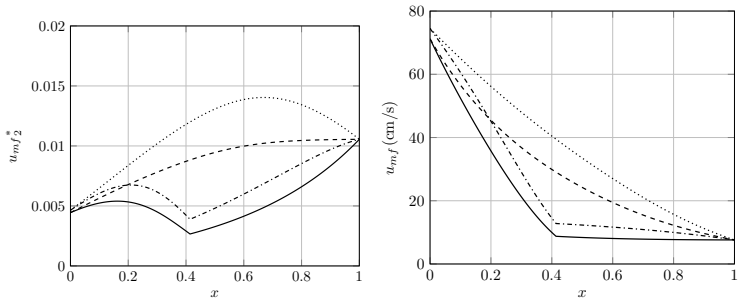

(e) (f)

$\rho_s = 2500\,\mathrm{kg/m^3}$, $w = 2$, and $r = 0.15$.

Figure 6: Comparison between scaled (a, c, e) and unscaled (b, d, f) minimum fluidisation velocities for sets of particle properties detailed in Tab. 1. The effects of inertial forces are included in the calculation of the minimum fluidisation velocities.

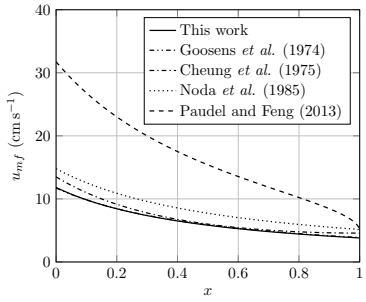

(a) $\rho_s = 1250\,\mathrm{kg/m^3}$, $w = 0.5$, $r = 0.8$ and $r = 1.0$.

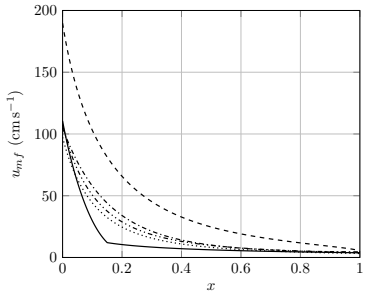

(b) $\rho_s = 1250\,\mathrm{kg/m^3}$, $w = 0.5$, and $r = 0.15$.

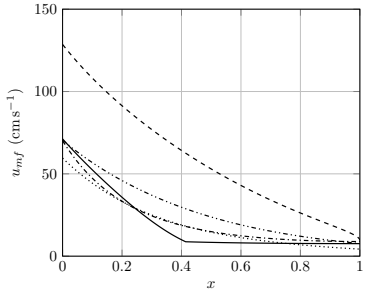

(c) $\rho_s = 2500\,\mathrm{kg/m^3}$, $w = 2$, and $r = 0.15$.

Figure 7: Comparison between various predictions of bed minimum fluidisation velocity u_{mf_1} for the sets of particle properties detailed in Tab. 1. Cheung *et al.*[3] is an empirical fit for which the minimum fluidisation velocities for when $x = 0$ and $x = 1$ were calculated using the Ergun equation and Goossens *et al.* [4] is the application of the Wen and Yu equation with mixture quantities. Noda *et al.* [6] and Paudel *et al.*[8] are modifications of the Goossens *et al.* approach with fitted changes to the numerical terms in the equation for biomass systems.

Table

Figures	w	r	d_s(µm)	d_l(µm)	ρ_s(kg/m^3)	ρ_l(kg/m^3)	Ar_s	Ar_l
Figs 6a, 6b	0.5	0.8	300	375	1250	2500	76	298
Fig. 6a, 6b, 7a	0.5	1	300	300	1250	2500	76	153
Fig. 6c, 6d, 7b	0.5	0.15	300	2000	1250	2500	76	45 300
Fig 6e, 6f, 7c	2	0.15	300	2000	2500	1250	153	22 600

Table 1: Table of properties for the particles used in the unscaled examples shown in Figs 6 and 7